HHS Public Access

Author manuscript

Clin Cancer Res. Author manuscript; available in PMC 2018 June 15.

Published in final edited form as:

Clin Cancer Res. 2017 June 15; 23(12): 3181–3190. doi:10.1158/1078-0432.CCR-17-0201.

Inhibition of age-related therapy resistance in melanoma by rosiglitazone-mediated induction of Klotho

Reeti Behera[1], **Amanpreet Kaur**[1,2], **Marie R. Webster**[1], **Suyeon Kim**[1], **Abibatou Ndoye**[1,2], **Curtis H. Kugel III**[1], **Gretchen M. Alicea**[1,2], **Joshua Wang**[1], **Kanad Ghosh**[1], **Phil Cheng**[3], **Sofia Lisanti**[1], **Katie Marchbank**[1], **Vanessa Dang**[1], **Mitchell Levesque**[3], **Reinhard Dummer**[3], **Xiaowei Xu**[4], **Meenhard Herlyn**[1], **Andrew E. Aplin**[5], **Alexander Roesch**[6], **Cecilia Caino**[1], **Dario C. Altieri**[1], and **Ashani T. Weeraratna**[1,*]

[1]The Wistar Institute, Philadelphia, Pennsylvania [2]University of the Sciences, Philadelphia, Pennsylvania [3]University of Zurich, Zurich, Switzerland [4]Department of Pathology, University of Pennsylvania [5]Sidney Kimmel Cancer Center, Thomas Jefferson University [6]Department of Dermatology, University Hospital, West German Cancer Center, University Duesburg-Essen, Essen, Germany

Abstract

Purpose—Aging is a poor prognostic factor for melanoma. We have shown that melanoma cells in an aged microenvironment, are more resistant to targeted therapy than identical cells in a young microenvironment. This is dependent on age-related secreted factors. Klotho is an age-related protein, whose serum levels decrease dramatically by age 40. Most studies on klotho in cancer have focused on the expression of klotho in the tumor cell. We have shown that exogenous klotho inhibits internalization and signaling of Wnt5A, which drives melanoma metastasis and resistance to targeted therapy. We investigate here whether increasing klotho in the aged microenvironment could be an effective strategy for the treatment of melanoma.

Experimental Design—PPARγ increases klotho levels, and is increased by glitazones. Using rosiglitazone, we queried the effects of rosiglitazone on Klotho/ Wnt5A crosstalk, in vitro and in vivo, and the implications of that for targeted therapy in young vs. aged animals.

Results—We show that rosiglitazone increases klotho and decreases Wnt5A in tumor cells, reducing the burden of both BRAF-inhibitor sensitive, and BRAF inhibitor-resistant tumors in aged, but not young mice. However, when used in combination with PLX4720, tumor burden was reduced in both young and aged mice, even in resistant tumors.

Conclusions—Using glitazones as adjuvant therapy for melanoma may provide a new treatment strategy for older melanoma patients who have developed resistance to vemurafenib. As klotho has been shown to play a role in other cancers too, our results may have wide relevance for multiple tumor types.

*To Whom Correspondence Should Be Addressed: Ashani T. Weeraratna, Ph.D., The Wistar Institute, Rm 452/454A, 3601 Spruce Street, Philadelphia, PA 19104, Office: 215 495-6937, Fax: 215 495-6938, aweeraratna@wistar.org.

COI: Ashani Weeraratna is on the Scientific Advisory Board of Phoremost Technologies.

Introduction

Dermal fibroblasts undergo age-related changes that result in altered secretory profiles. We have recently shown that these age-related changes can drive melanoma progression, and therapy resistance. We found that one of the ways in which the aged microenvironment promoted metastasis was via secretion of an inhibitor of canonical Wnt signaling, sFRP2. sFRP2 secreted by aged dermal fibroblasts suppressed β-catenin signaling in melanoma cells. The loss of β-catenin signaling has been associated with a increase in metastatic capacity of melanoma cells, as well as a decrease in sensitivity to vemurafenib. We found this to be true for melanoma cells in an aged microenvironment as well, such that the restoration of β-catenin signaling by anti-sFRP2 antibody in vivo re-sensitized tumors to vemurafenib, and decreased their metastatic ability. In melanoma, the secreted non-canonical Wnt signaling molecule, Wnt5A, also drives the metastatic progression of melanoma (1) and resistance to targeted therapy, in part by inhibiting β-catenin signaling (2). Wnt5A is therefore significantly associated with poorer prognosis in melanoma. We have recently asked what factors might regulate Wnt5A, and we, and others, have identified the anti-aging hormone klotho as a regulator of Wnt signaling (3, 4).

Klotho is a circulating serum factor, which is lost during aging. Overexpression of klotho in transgenic mice promotes longevity (5). Conversely, the knockout of klotho results in a complex premature aging phenotype, where mice that are born phenotypically normal develop atherosclerosis, osteoporosis, skin atrophy and bone degeneration. Klotho has also been shown to decrease Wnt signaling (3). We discovered that Wnt5A is bound to the surface of melanoma cells by heparan sulfate proteogylcans (6), and klotho, which has sialidase activity (7), cleaves Wnt5A from the proteoglycans, such that it cannot be internalized and signal (4). Once this occurs, Wnt5A mRNA expression also decreases, as Wnt5A increases PKC, which in turn signals to stabilize Wnt5A mRNA. Klotho therefore affects both Wnt5A internalization and mRNA expression, and treatment of Wnt5A-high cells with recombinant klotho significantly inhibits their invasion (4).

In addition to its sialidase activities, klotho plays essential roles in maintaining phosphate homeostasis, inhibiting oxidative stress, suppressing cellular senescence and modulating insulin receptor signaling (8–11). The loss of klotho is thought to correspond either directly or indirectly to increased insulin resistance, which is associated with diabetes (5). Recently, there has been much interest in using anti-diabetic drugs to treat melanoma. Drugs such as metformin and phenformin have been suggested because they affect mitochondrial biogenesis and changes in mitochondrial biogenesis affect melanoma cell response to vemurafenib, and contribute to drug resistance (12, 13).

Another class of drugs used to treat diabetes is the glitazones, which are agonists of the peroxisome proliferator-activated receptor, PPARγ, a nuclear hormone receptor that controls the transcription of multiple genes involved in lipid biogenesis and metabolism (14). Klotho is a transcriptional target of PPARγ, such that PPARγ increases klotho mRNA (15). Wnt5A has recently been shown to inhibit expression of PPARγ via the activation of CAMKII (16). We previously reported that Wnt5A also inhibited klotho, largely at the mRNA level, but at the time did not have a mechanism by which it did so. We hypothesized that Wnt5A may be

able to repress klotho expression via CAMKII- mediated suppression of PPARγ. Here we test and confirm this hypothesis. We further show that using available PPARγ agonists, such as rosiglitazone (trade name Avandia), can increase serum levels of klotho in the blood and in the tumor microenvironment, and decrease Wnt5A. Intriguingly we also find that rosiglitazone decreases the growth of BRAF resistant melanomas in aged, but not young mice.

Methods

CELL CULTURE

WM858, WM793, WM164 and 1205LU cells were maintained in MCDB153 (Sigma, St Louis, MO)/ L-15 (Cellgro, Manassas, VA) (4:1 ratio) supplemented with 2% FBS and 1.6 mM CaCl2 (Tumor growth media). WM983B cells were maintained in DMEM (Invitrogen, Carlsbad, CA), supplemented with 5% FBS, 100 units/ml penicillin and streptomycin and 4 mM L-glutamine. The PLX4720 resistant cell lines were cultured in media same as the parent lines in presence of PLX4720 (Chemietek). FS5, FS4, cells were maintained in RPMI (Invitrogen, Carlsbad, CA), supplemented with 10% FBS, 100 units/ml penicillin and streptomycin and 4 mM L-glutamine. Yumm1.7 melanoma cells derived from the BRAFV600E/PTEN−/−/CDKN2A−/− mouse model of melanoma and human fibroblasts were maintained in DMEM, supplemented with 10% FBS, 100 units/ml penicillin and streptomycin and 4 mM L-glutamine. Yumm1.7 cells were cultured to resistance in 10μM PLX4720. Keratinocytes were maintained in keratinocyte SFM supplemented with human recombinant Epidermal Growth Factor 1–53 (EGF 1–53) and Bovine Pituitary Extract (BPE) (Invitrogen). All the cell lines were cultured at 37°C in 5% CO2. Cell stocks were fingerprinted using AmpFLSTR® Identifiler® PCR Amplification Kit from Life Technologies TM at The Wistar Institute Genomics Facility. Although it is desirable to compare the profile to the tissue or patient of origin, our cell lines were established over the course of 40 years, long before acquisition of normal control DNA was routinely performed. However, each STR profile is compared to our internal database of over 200 melanoma cell lines, as well as control lines, such as HeLa and 293T. STR profiles are available upon request. Cell culture supernatants were mycoplasma tested using a Lonza MycoAlert assay at the University of Pennsylvania Cell Center Services.

TREATMENTS

Cells were treated with 100 ng/ml of recombinant Wnt5A (R&D Systems, cat. no. 645WN010CF) for 16 h or 10ng/ml of recombinant klotho (R&D Systems, cat. no. 5334-KL-025) for 48 h. KN93 (Cayman, cat. no. 13319) was used at a final concentration of 10μM and Rosiglitazone (Sigma-Aldrich, cat. no. R2408-50MG) at 10μM for 48 h unless otherwise stated. BRAF resistance subclones were seeded overnight in the absence of PLX4720 and then treated as indicated.

WESTERN BLOTTING

Western blotting was done as described in (17). Briefly, total protein lysate of 50–65μg was run on 4–12% NuPAGE Bis Tris gel (Invitrogen, cat no. NW 041222BOX), transferred onto PVDF membrane using iBlot 2, Life technologies and blocked in 5%milk/TBST. To analyze

level of secretory klotho, conditioned media from fibroblasts was run on 4–12% NuPAGE Tris gel and total protein lysate from the fibroblasts was used to probe for HSP90 as loading control. Primary antibodies were used at the following concentrations: biotinylated Wnt5A (500 ng/ml; R&D Systems, cat. no. BAF645), Klotho (1:500; abcam, cat. no. ab98111), HSP90 (1:4000; Cell Signaling, cat. no. 4877S), CAMKII (1:500; Cell Signaling, cat. no. 3362S), CAMKII alpha/delta (p Thr286) (1:500; NBP1-51462, Novus), pERK (1:500; Cell Signaling, cat no. 4370S), ERK (1:500; Cell Signaling, cat no. 4696S). All primary antibodies were diluted in 5% milk/TBST and incubated overnight at 4°C. The membranes were washed in TBST and probed with the corresponding HRP-conjugated secondary antibody (0.2–0.02 μg/ml of anti-mouse, streptavidin, or anti-rabbit). Proteins were visualized using ECL prime (Amersham, Uppsala, Sweden) or Luminata Crescendo (Millipore, Billerica, MA, USA).

ORGANOTYPIC 3D SKIN RECONSTRUCTS

Organotypic 3D skin reconstructs were generated as previously described (18). Briefly, 6.4 x 104 fibroblasts were plated in each insert on top of the acellular layer (BD, cat. no. 355467 and Falcon, cat. No. 353092) and incubated for 45 min at 37°C in a 5% CO2 tissue culture incubator. The tissue culture trays were filled with DMEM containing 10% FBS and incubated for 4 days. Reconstructs were then incubated for 1 h at 37°C in HBSS containing 1% dialyzed FBS (wash media). Washing media was removed and replaced with reconstruct media. Keratinocytes (4.17 x 105) and melanoma cells (8.3 x 104) were added to the inside of each insert. Media was changed every other day until day 18, reconstructs were then harvested, fixed in 10% formalin, paraffin embedded, sectioned and stained.

IMMUNOHISTOCHEMISTRY (IHC)

Immunohistochemistry was performed on paraffin embedded sections as described previously (18). Briefly, Paraffin embedded sections were rehydrated through a xylene and alcohol series rinsed in H2O and washed in PBS. Antigen retrieval was performed by steaming for 20 min in target retrieval buffer (Vector Labs, Burlingame, CA) and steamed for 20 min. Samples were blocked in a peroxidase blocking buffer (Thermo Scientific) followed by Protein block (Thermo Scientific) and incubated in appropriate primary antibody diluted in antibody diluent (S0809, Dako) at 4°C overnight in a humidified chamber. Samples were then incubated in biotinylated anti-rabbit or polyvalent secondary antibody (Thermo Scientific) followed by streptavidin-HRP solution. Samples were then washed in PBS and incubated in 3-Amino-9-Ethyl-l-Carboazole (AEC) chromogen. Finally, samples were washed in H2O, incubated in Meyer’s hematoxylin for 1 min, rinsed in cold H2O, and mounted in Aquamount. Patient samples were collected under IRB exemption approval for protocol #EX21205258-1.

IMMUNOFLUORESCENCE (IF)

Cells were seeded onto glass cover slips and incubated overnight. These cells were then treated with fibroblast conditioned media, KN93 or Rosiglitazone with the indicated dose for 48 h. Cells were fixed with 4% paraformaldehyde, permeabilized with 0.2% TritonX-100, blocked with 1% BSA and stained for primary antibodies as previously described (18). When staining for klotho cells were not permeabilized. For immunofluorescence staining in

the 3D skin reconstructs, the paraffin embedded sections were rehydrated, processed for antigen retrival and blocked as described for IHC. Primary antibodies were used at the following concentrations: Klotho (1:150), PPARγ (1:100, abcam, cat. No. ab19481), Wnt5A (1:50), HMB45 (1:50, abcam, cat. No. ab787) and incubated at 4°C overnight. Cells were washed in PBS and incubated with the appropriate secondary antibody (1:2000, Invitrogen) for 1 h at room temperature and mounted in Prolong Gold anti-fade reagent containing DAPI (Invitrogen). Images were captured on a Leica TCS SP5 II scanning laser confocal system.

LENTIVIRAL INFECTION

shRNA against human klotho was obtained from Sigma-Aldrich, KL MISSION shRNA Bacterial Glycerol Stock. Klotho shRNA clones used were: TRCN0000158823 and TRCN0000160036. Lentiviral production was performed as described previously (18). Briefly, 293T cells were co-transfected with Klotho shRNA vector and lentiviral packaging plasmids (pCMV-dR8.74psPAX2, pMD2.G). The supernatant containing virus was harvested at 36 and 60 hours, combined and filtered through a 0.45μm filter and stored in −80 degrees till further use. For transduction, the cells were layered overnight with lentivirus containing 8 μg/ml polybrene. The cells were allowed to recover for 24 hours and then selected using 1μg/ml puromycin.

siRNA TRANSFECTION

KL siRNA and negative control siRNA (100nM, ambion) were transfected into cells using Lipofectamine 2000 (Thermo Fisher Scientific) as per manufacturer's protocol.

MITOCHONDRIAL STAINING

Melanoma cells treated with indicated conditions were seeded onto a 384 well plate at 3000 cells/well in triplicate (PerkinElmer cell carrier). For analyzing mitochondrial mass, cells were incubated with MitoTracker® Green FM (M7514, ThermoFisher Scientific) at 1μM concentration for 1 h. To analyze production of superoxide by mitochondria, cells were incubated with MitoSOX™ Red reagent (M36008, ThermoFisher Scientific) at a final concentration of 5μM for 10 min, washed extensively and were imaged using PerkinElmer Operetta. The fluorescent signal was quantified using Harmony 3.0 software. Readings were normalized to cell number which was determined by Hoescht staining (Hoechst 33342, Invitrogen). Cells seeded on coverslips were also stained with MitoTracker® Red CM-H2Xros (M7513, Thermofisher Scientific) at 1μM concentration for 1 h, fixed with formaldehyde 4% and mounted in Prolong Gold anti-fade reagent. Images were captured on a Leica TCS SP5 II scanning laser confocal system. Fluorescence were normalized to cell number.

TCGA DATABASE ANALYSIS

The RNAseq and Clinical data set for skin cutaneous melanoma (19) was downloaded from TCGA (http://cancergenome.nih.gov/). Patient ages were group into 10 year age ranges. Patient sample information is included in Supplementary Table 1.

REAL TIME PCR

RNA was extracted using Trizol (Invitrogen) and RNeasy Mini kit (Qiagen) as previously described (18). cDNA was prepared using iscript cDNA synthesis kit (Bio-Rad, cat. No. 1708891). Gene expression was quantified using SYBR green method of qPCR and mRNA levels were compared to standard curves. qPCR was performed on an ABI StepOnePlus sequence detection system using fast conditions and samples were normalized against the 18S gene, using Universal 18S primers (Invitrogen, cat. No. AM1718). Expression was calculated using the standard curve method according to the manufacturer's protocol (Perkin Elmer, Waltham, MA). The sequences for primers are Klotho forward primer: GCTCTCAAAGCCCACATACTG; Klotho reverse primer: GCAGCATAACGATAGAGGCC Wnt5a forward primer: AGGGCTCCTACGAGAGTGCT; Wnt5a reverse primer: GACACCCCATGGCACTTG.

CELL VIABILITY ASSAY (MTS)

Cell viability was determined using CellTiter 96 Aqueous One Solution Cell Proliferation Assay according to manufacturers protocol. Briefly, cells were seeded in flat bottom 96-well plates and allowed to adhere overnight. The next day, cells were treated with the indicated drugs for indicated time period. Following treatments, cells were incubated with MTS dye (20 μl/well) for 2 h. Absorbance was determined at 490nm using an EL800 microplate reader (BioTek, Winooski, VT). The percent cell viability was calculated by converting the experimental absorbance to percentage of control and plotted vs drug concentration. The values were then analyzed using a nonlinear dose-response analysis in GraphPad Prism.

IN VIVO TUMOR BURDEN ASSAY

All animal experiments were approved by the Institutional Animal Care and Use Committee (IACUC) (IACUC #112503X_0) and were performed in an Association for the Assessment and Accreditation of Laboratory Animal Care (AAALAC) accredited facility. YUMM1.7 parental or YUMM1.7_BR (2.5 x 105 cells) were injected subcutaneously into young (6 week old) and aged (52 week old) C57/BL6 mice (Charles River). Tumor sizes were measured every 3–4 days using digital calipers, and tumor volumes were calculated using the following formula: volume = 0.5 x (length x width2). When resulting tumors reached 200 mm3, mice were fed with either AIN-76A chow or AIN-76A chow containing 417 mg/kg PLX4720. Time-to-Event (survival) was determined by a 5-fold increase in baseline volume (~1000 mm^3) and was limited by the development of skin necrosis. For treatment with recombinant mouse Klotho (R&D systems, Cat. No. 1819KL) or Rosiglitazone, mice were injected intraperitoneally with recombinant Klotho, 0.02mg/Kg every 2 days or with Rosiglitazone, 10mg/Kg every other day. To analyze klotho levels in serum, serum was isolated from blood collected by sub-mandibular bleeding and Klotho levels were analyzed by western blotting. At the end of experiment mice were euthanized, tumors were harvested and a portion of the tumors were embedded in paraffin and sectioned.

STATISTICAL ANALYSIS

For in vitro studies, a Student's t-test or Wilcoxon rank-sum test (Mann Whitney) was performed for two-group comparison. Estimate of variance was performed and parameters

for the t-test were adjusted accordingly using Welch's correction. ANOVA or Kruskal-Wallis test with post-hoc Bonferroni's or Holm-Sidak's adjusted p-values was used for multiple comparisons. For in vivo studies, repeated measures analysis of variance (Anova) was calculated between samples. Holm Sidak correction was performed. For other experiments, Graphpad/Prism6 was used for plotting graphs and statistical analysis. Data was represented as +/− SEM. Significance was designated as follows: *, $p<0.05$; **, $p<0.01$; ***, $p<0.001$.

Results

Manipulation of klotho in dermal fibroblasts affects Wnt5A expression in melanoma cells

Klotho expression is decreased in aged human skin (Figure 1a). We have recently shown that aged dermal fibroblasts can drive the metastasis and therapeutic resistance of melanoma largely through secreted factors. To investigate if the loss of klotho from fibroblasts contributes to the increased aggression and therapy resistant phenotype of melanoma cells in the aged microenvironment, we assayed dermal fibroblasts derived from non-melanoma, healthy donors who were either young (25–35 years old) or aged (55–65 years old) for expression of klotho. All fibroblast experiments were normalized to cell number. As expected, aged dermal fibroblasts demonstrated a decrease in klotho expression as compared to young fibroblasts, as measured by RT-PCR, Western analysis, (Figure 1b,c), and immunofluorescent analysis (Supplementary Figure 1a). Further, klotho expression was also decreased in the serum of aged mice, as measured by ELISA (Supplementary Figure 1b). In skin reconstructs built with aged and young fibroblasts, young fibroblasts continued to express klotho, whereas aged fibroblasts did not (Supplementary Figure 1c). Melanoma cells, surprisingly, recapitulated the age-related klotho expression of fibroblasts: if young fibroblasts were present in the skin reconstruct, melanoma cells in the proximity also expressed klotho. If aged fibroblasts were present, melanoma cells expressed lower levels of klotho (Figure 1d). TCGA analysis of melanoma samples revealed that klotho is indeed decreased in melanoma patients as they age. The difference is most significant under 40 (the age where klotho is lost in the serum) and over 55 (where the incidence of melanoma increases rapidly), however expression decreases steadily by decade (Supplementary Figure 1d, patient information provided in Supplementary Table 1).

Since we have previously shown that exogenous klotho affects Wnt5A internalization and expression, we asked whether differences in the amount of klotho secreted from young vs. aged fibroblasts affected Wnt5A accordingly in melanoma cells. To confirm that any effects observed were fibroblast-related, we treated melanoma cells with media from young and aged fibroblasts, as well as with un-conditioned media with and without 10% fetal bovine serum (FBS). As expected, in the melanoma cells treated with serum-free media, Wnt5A was elevated (Figure 1e). Consistent with our hypothesis, Wnt5A expression was low in melanoma cells treated with both serum-containing media and media from young fibroblasts. However, when we tested the serum-containing media for klotho we found that it contained klotho (data not shown). In contrast, aged fibroblast media resulted in an elevated level of Wnt5A expression (Figure 1e, Supplementary Figure 1e). Melanoma cells in aged fibroblast conditioned media also have less klotho mRNA as compared to the cells in young fibroblast conditioned media (Supplementary Figure 1 f).

We next observed Wnt5A regulation by the aged microenvironment in artificial skin reconstructs made with young or aged fibroblasts, into which we put identical melanoma cell lines. As noted above (Figure 1d) melanoma cells recapitulate the klotho expression of the fibroblasts, such that melanoma cells in reconstructs made with young fibroblasts express klotho, and melanoma cells in reconstructs made with aged fibroblasts express less klotho. Consistent with our hypothesis that klotho modulates Wnt5A expression, in skin reconstructs made with aged fibroblasts and melanoma cells, Wnt5A was increased in melanoma cells, compared to identical skin reconstructs built with young fibroblasts (Figure 1f, additional cell line, Supplementary Figure 1i, j). To determine whether this differential Wnt5A expression could be altered by manipulating klotho in young and aged fibroblasts, we knocked down klotho using sh_RNA against klotho (sh_klotho) in young fibroblasts (Supplementary Figure 1g, h) and observed an increase in Wnt5A in melanoma cells exposed to sh_klotho fibroblast media. Conversely, treating aged fibroblasts with recombinant klotho (rklotho) decreased Wnt5A in melanoma cells exposed to rklotho-supplemented aged media (Figure 1g). We confirmed this result in skin reconstructs built using young fibroblasts treated with either a control (scrambled) shRNA, or with a klotho shRNA. In the reconstructs built with the klotho knockdown fibroblasts, the levels of klotho in the melanoma cells decrease (Figure 1h) and the level of Wnt5A increases (Figure 1i), mimicking the aged fibroblast conditions. Together these data indicate that the loss of klotho in the aged microenvironment, specifically in dermal fibroblasts, increases Wnt5A in melanoma cells. We have shown extensively that Wnt5A is involved in multiple aspects of tumor progression. Therefore, reconstitution of Wnt5A upon klotho loss during aging may be another mechanism leading to the increased aggression of melanoma in the elderly.

Wnt5A suppresses klotho via CAMKII mediated inhibition of PPARγ

We previously showed that Klotho acts as a sialidase, cleaving Wnt5A away from the surface of melanoma cells. We next wanted to determine the mechanism by which Wnt5A can regulate klotho. Klotho is a target of PPARγ, a regulator of fatty acid storage and glucose metabolism (15). PPARγ is phosphorylated and degraded by the activation (phosphorylation) of CAMKII, which in turn is a direct target of Wnt5A (16). Thus, we hypothesized that Wnt5A regulates klotho expression via CAMKII mediated degradation of PPARγ (outlined in Figure 2a). Indeed, treatment of melanoma cells with rWnt5A increased CAMKII phosphorylation (Figure 2b) and decreased PPARγ and klotho (Figure 2c). Conversely, when aged fibroblasts were treated with the CAMKII inhibitor KN93, mRNA expression of klotho was increased (Figure 2d), as was protein expression of PPARγ (Figure 2e). Even at the highest doses, KN93 was not toxic to fibroblasts (Supplementary Figure 2a, b). To determine whether KN93 had similar effects on melanoma cells, we treated melanoma cells with KN93 (10μM, 48h) and demonstrated that PPARγ and klotho were restored (Figure 2f, g). Consistently, exploration of PPARγ expression levels in the TCGA database revealed that, like klotho, PPARγ levels were decreased in older melanoma patients (Supplementary Figure 2c, aged vs. young at different decades of life).

As our data above suggested that activation of PPARγ should increase klotho, and regulate Wnt5A, we treated aged fibroblasts with the PPARγ agonist rosiglitazone, which increased PPARγ, and klotho (Figure 2h, i). Melanoma cells treated with rosiglitazone demonstrated a

decrease in the secreted form of Wnt5A in the lysate (Supplementary Figure 2d, upper band). As in fibroblasts, we observed increases in both PPARγ and klotho in melanoma cells treated with rosiglitazone (Supplementary Figure 2e). Like KN93, Rosiglitazone was not toxic to either fibroblasts or melanoma cells at high doses (Supplementary Figure 2f, g). To translate these findings in vivo, we used Yumm1.7 melanoma cells derived from the $BRAF^{V600E}/PTEN^{-/-}/CDKN2A^{-/-}$ mouse model of melanoma, and injected them into C57BL/6 mice. When tumors were palpable, we treated one set of aged mice with 10mg/kg of rosiglitazone and one set with 0.02mg/kg of recombinant klotho, and treated a third set with PBS/DMSO vehicle control. Tumor burden was significantly reduced as compared to control by treatment with either rosiglitazone or recombinant klotho (Figure 2j). Treatment of aged mice with rosiglitazone or recombinant klotho decreased Wnt5A and increased klotho levels in the tumor (Figure 2k). Together these data suggest that using rosiglitazone as an agent to increase PPARγ and klotho can decrease Wnt5A and inhibit tumor growth in an aged microenvironment.

Rosiglitazone-mediated inhibition of Wnt5A can inhibit growth of BRAF-inhibitor resistant cells

One of the first line therapies for melanoma is the drug vemurafenib, which targets a mutant BRAF protein ($BRAF^{V600E}$). Our previous work demonstrated that Wnt5A can promote resistance to targeted therapy in melanoma (2, 17), and we support this by showing that knockdown of Wnt5A can increase the sensitivity of melanoma cells to PLX4720, the tool compound for Vemurafenib (Supplementary Figure 3a, b). Further, Wnt5A is more highly secreted by aged as compared to young fibroblasts (Supplementary Figure 3c), which is in keeping with our previous data showing that melanomas in an aged microenvironment are more resistant to vemurafenib, largely due to changes in Wnt signaling (18). Importantly, it has been shown that Wnt5A can signal to activate ERK, and CAMKII, also a target of Wnt5A, activates the Raf signaling pathway further. This represents a way to maintain activation of the MAPK pathway, regardless of mutational status. To determine if manipulating this pathway in melanoma cells could affect resistance of melanoma cells to BRAF inhibition, we created a resistant subclone of Yumm1.7 cells that we could use in vivo. These subclones are as resistant in vitro to PLX4720 (the tool compound for vemurafenib) as are WM983B BRAF inhibitor-resistant subclones (Supplementary Figure 4a). Next we analyzed the Yumm1.7, WM983B, WM793 and their resistant subclones for Wnt5A and PO_4-ERK. Each of these cell lines bears a different set of mutations (Supplementary Table 2). In each case, both Wnt5A and PO_4-Erk were elevated (Figure 3a). This was also concomitant with the loss of klotho and PPARg expression (Supplementary Figure 4b–f). We then asked whether increasing klotho via rosiglitazone reduced PO_4-Erk signaling, via downregulation of Wnt5A. PO_4-Erk is decreased in BRAF-resistant cell lines after treatment with rosiglitazone (Figure 3b) and this is concomitant with the decrease in Wnt5A (Supplementary Figure 4g). KN93 is similarly able to cause decreases in both PO_4-Erk and Wnt5A (Supplementary Figure 4h). We then asked whether transcriptionally silencing klotho would prevent rosiglitazone from decreasing ERK activity and decreasing Wnt5A. Knocking down klotho in young fibroblasts increased PO_4-Erk and Wnt5A (Supplementary Figure 4i). In melanoma cells treated with rosiglitazone, there is a reduction of both Wnt5A and PO_4-ERK. However, first knocking down klotho results in activated Erk,

and sustained Wnt5A signaling, even in the presence of rosiglitazone (Figure 3c, Supplementary Figure 4j). These data suggest that Rosiglitazone is mediating its effects on the Erk pathway via klotho-mediated suppression of Wnt5A.

We have previously shown that tumors in an aged microenvironment are more resistant to targeted therapy. Therefore, we examined whether increasing klotho in the microenvironment could affect response to PLX4720. We took aged fibroblasts, and treated them with rosiglitazone. We then exposed BRAF resistant melanoma cells to the media from the treated fibroblasts, in the presence or absence of PLX4720. Western analysis of PO_4-ERK (Figure 3d) demonstrates that rosiglitazone treatment of the fibroblasts also reduces PO_4-ERK levels in melanoma cells. We have shown that mitochondrial ROS marks response to PLX4720, such that increases in mito-Sox correlate to increased resistance (Supplementary Figure 5a,b). As with PO_4-ERK, mito-sox activity is lowered by rosiglitazone in melanoma cells incubated with aged fibroblasts, both in the presence and absence of PLX4720 (Figure 3e, Supplementary Figure 5c–e).

Taken together these data suggested that targeting klotho in both the melanoma cells and the microenvironment in aged mice should have effects on BRAFi resistant melanomas. To test this hypothesis in vivo, we treated Yumm1.7BR resistant cells with rosiglitazone or klotho, in the presence and absence of PLX4720 and demonstrated that these treatments decreased Wnt5A (Supplementary Figure 5f). Yumm1.7BR cells were injected subcutaneously into aged mice. Treatment with PLX4720 alone did not affect tumor growth compared to controls, whereas treatment with rosiglitazone alone, and the combination of rosiglitazone and PLX4720, impeded the rate of tumor growth (Figure 3f). The combination was not more effective than rosiglitazone alone. To determine if these results differed in young mice, we repeated the identical experiments in 8-week old mice. In young mice, Yumm1.7BR cells re-acquired sensitivity to PLX4720, in keeping with previous data from our lab that indicated that melanoma cells are more sensitive to BRAFi in a young microenvironment (18). Intriguingly, treating young mice with rosiglitazone alone accelerated tumor growth; however, rosiglitazone + PLX4720 decreased tumor burden compared to PLX4720 alone (Figure 3g). To assay whether klotho was differentially increased in Yumm1.7BR cells in rosiglitazone-treated aged vs. young mice, we examined the serum of mice for klotho expression, and stained the tumors for klotho. In aged mice, klotho expression is low in Yumm 1.7BR tumors and in serum, and klotho increases in aged mice upon treatment with rosiglitazone (Figure 3h, left). In young mice however, klotho is high at baseline in both the tumor and mouse serum, and elevated even further by rosiglitazone treatment (Figure 3h, right). These data indicate that rosiglitazone may be a unique therapy for older patients, and while it cannot re-sensitize melanoma cells to vemurafenib, it can still reduce tumor burden, both in BRAF-inhibitor sensitive and resistant cells in aged animals. Rosiglitazone may be a viable alternate strategy to reduce tumor burden in older patients who have developed resistance to BRAF inhibitors. Our data suggest also that since PO_4-Erk is reduced by direct treatment of melanoma cells with rosiglitazone, the right dosing schedule of rosiglitazone and PLX4720 may provide additional benefit in combination with BRAF inhibitors in young patients as well, which will be the subject of further study in our laboratory.

Discussion

The role of klotho in aging has been well documented. The loss of klotho has also been implicated in the progression of multiple tumor types, including lung (20), cervical (21) and gastric cancer (22). In addition, we have shown that treating melanoma cells with recombinant klotho can reduce their invasion by inhibiting Wnt5A signaling, which is elevated in metastatic melanoma cells. We have also shown that, in addition to promoting metastasis, Wnt5A can increase resistance to vemurafenib. Maintaining klotho in aged patients then, could have the twin benefits of decreasing metastasis and inhibiting therapy resistance. Since klotho is lost during aging, and we have recently shown that aging promotes melanoma metastasis and therapy resistance (18), here we asked whether klotho loss in the aged microenvironment, specifically in fibroblasts, promotes Wnt5A expression and affects therapy resistance. In this study we confirm that klotho is decreased in the aged skin microenvironment, and manipulation of klotho in aged and young dermal fibroblasts affects Wnt5A expression in melanoma cells. We also show, for the first time, that Wnt5A can regulate klotho and that it does so by CAMKII-mediated suppression of PPARγ. When Wnt5A is absent, PPARγ activation increases transcription of klotho.

Because some anti-diabetic drugs (e.g. metformin) have activity against melanoma (23), and because some of these medications are PPARγ agonists, there has been much interest in the use of PPARγ agonists to treat cancer. However, the studies performed so far provide conflicting data as to whether PPARγ agonists are beneficial. In colon cancer, studies indicate that malignancy can be reversed by rosiglitazone, pioglitazone and other thiazolidinediones (TZD) (24–26), but Phase II clinical trials do not support this (27). Similarly, in breast cancer, late-stage tumors are not affected by TZD. However, a more recent study has shown that if the glitazone is administered earlier, to less aggressive tumors, i.e., HER2+ breast cancer, then it does have protective effects (28). In the current study, we identify yet another parameter that may affect response to glitazones, and that is age. We show that rosiglitazone can increase levels of klotho in the serum of aged mice bearing melanoma, and that this translates to an inhibition of tumor growth similar to treating mice directly with klotho. Treating BRAF inhibitor resistant cells with rosiglitazone reduces ROS in the mitochondria, and kills tumor cells. While we cannot claim that rosiglitazone re-sensitizes cells to vemurafenib, because at the doses used there was no added benefit to rosiglitazone + PLX4720 vs. rosiglitazone alone, it is quite clear that rosiglitazone may prove to be effective against BRAFi resistant melanoma, when other options have failed. Similarly, increasing klotho with rosiglitazone inhibits the growth of both BRAFi-sensitive and BRAFi-resistant melanoma equally effectively in aged animals.

Increasing rosiglitazone increased klotho levels, decreased Wnt5A and decreased tumor burden in aged mice. However, this was not the case in young mice, and we were fascinated to find that treatment with rosiglitazone differed in young vs. aged mice. First, we have recently shown that changes in the aged microenvironment (e.g., increases in ROS and sFRP2) can drive increased resistance to targeted therapy (18). In that study, placing PLX4720-sensitive tumors in aged mice increased their ability to resist therapy. Here we show that the opposite is also true, i.e., that placing resistant tumors in young mice, slightly, but significantly, increases their sensitivity to PLX4720. Further, the combination of

PLX4720 and rosiglitazone is effective in young mice, and unlike in aged mice, rosiglitazone appears to sensitize tumors to PLX4720. We have shown in this study that treatment of melanoma with rosiglitazone lowers PO_4-Erk levels, which may be enough in the young microenvironment to further sensitize melanomas to PLX4720. However, rosiglitazone alone is ineffective in treating resistant tumors in young animals, and actually increases tumor burden in young mice. The mechanism for this is not entirely clear, but may be due to a klotho threshold present in cells, which determines their susceptibility to PLX4720 and other MAPK targeting agents. In this case, endogenous levels of klotho in young mice may partially re-sensitize resistant tumors to targeted therapy, and increasing klotho with rosiglitazone in aged animals where klotho is endogenously low can decrease the growth of resistant tumors. However, raising klotho further in young animals does not serve to reduce tumor burden, presumably because klotho levels in young animals already surpass the threshold. In addition, increasing klotho too much may increase proliferation of the tumor, as klotho is known to increase cellular proliferation (29). If this is the case, as suggested by the accelerated tumor growth in the rosiglitazone-treated young mice, the age-specific nature of this therapy might serve to explain some of the observed discrepancies in studies analyzing the role of PPARγ agonists in the therapy of breast and colon cancer. Age may play an important role in determining which patients should receive rosiglitazone as therapy for melanoma, and since klotho is secreted in the serum, it should be relatively simple to determine which patients might benefit from rosiglitazone therapy, and which would not. Understanding the role that the aged microenvironment plays in modulating cell fates like metastasis and therapy resistance is critical for guiding therapy in older patients.

Supplementary Material

Refer to Web version on PubMed Central for supplementary material.

Acknowledgments

We thank Dr. Gideon Bollag of Plexxikon for PLX4720. We thank Dmitry Gourevitch of the Wistar Histology Core, and Fred Keeney of the Wistar Imaging facility. This work was supported in part by: RO1 CA174746-01 (ATW, RB), P01 CA 114046-06 (ATW, MH), T32 CA 9171-36 (MRW, CHKIII), a MRF Established Investigator award (ATW), an ACS-IRG award (ATW), a Miriam and Sheldon Adelson Research Foundation Award (AEA, MH), P50 CA174523-01 (ATW, XX, MH) and R01-CA1826635 (AEA). Core facilities at the Wistar Institute are supported by the CCSG grant P30 CA010815.

References

1. Dissanayake SK, Wade M, Johnson CE, O'Connell MP, Leotlela PD, French AD, et al. The Wnt5A/protein kinase C pathway mediates motility in melanoma cells via the inhibition of metastasis suppressors and initiation of an epithelial to mesenchymal transition. J Biol Chem. 2007; 282:17259–71. [PubMed: 17426020]
2. O'Connell MP, Marchbank K, Webster MR, Valiga AA, Kaur A, Vultur A, et al. Hypoxia induces phenotypic plasticity and therapy resistance in melanoma via the tyrosine kinase receptors ROR1 and ROR2. Cancer Discov. 2013; 3:1378–93. [PubMed: 24104062]
3. Liu H, Fergusson MM, Castilho RM, Liu J, Cao L, Chen J, et al. Augmented Wnt signaling in a mammalian model of accelerated aging. Science. 2007; 317:803–6. [PubMed: 17690294]
4. Camilli TC, Xu M, O'Connell MP, Chien B, Frank BP, Subaran S, et al. Loss of Klotho during melanoma progression leads to increased filamin cleavage, increased Wnt5A expression, and

enhanced melanoma cell motility. Pigment Cell Melanoma Res. 2011; 24:175–86. [PubMed: 20955350]

5. Kuro-o M. Klotho and aging. Biochim Biophys Acta. 2009; 1790:1049–58. [PubMed: 19230844]
6. O'Connell MP, Fiori JL, Kershner EK, Frank BP, Indig FE, Taub DD, et al. Heparan sulfate proteoglycan modulation of Wnt5A signal transduction in metastatic melanoma cells. J Biol Chem. 2009; 284:28704–12. [PubMed: 19696445]
7. Cha SK, Ortega B, Kurosu H, Rosenblatt KP, Kuro OM, Huang CL. Removal of sialic acid involving Klotho causes cell-surface retention of TRPV5 channel via binding to galectin-1. Proc Natl Acad Sci U S A. 2008; 105:9805–10. [PubMed: 18606998]
8. de Oliveira RM. Klotho RNAi induces premature senescence of human cells via a p53/p21 dependent pathway. FEBS Lett. 2006; 580:5753–8. [PubMed: 17014852]
9. Hu MC, Shi M, Zhang J, Quinones H, Griffith C, Kuro-o M, et al. Klotho deficiency causes vascular calcification in chronic kidney disease. J Am Soc Nephrol. 2011; 22:124–36. [PubMed: 21115613]
10. Taketani Y, Shuto E, Arai H, Nishida Y, Tanaka R, Uebanso T, et al. Advantage of a low glycemic index and low phosphate diet on diabetic nephropathy and aging-related diseases. J Med Invest. 2007; 54:359–65. [PubMed: 17878688]
11. Wolf I, Levanon-Cohen S, Bose S, Ligumsky H, Sredni B, Kanety H, et al. Klotho: a tumor suppressor and a modulator of the IGF-1 and FGF pathways in human breast cancer. Oncogene. 2008; 27:7094–105. [PubMed: 18762812]
12. Cierlitza M, Chauvistre H, Bogeski I, Zhang X, Hauschild A, Herlyn M, et al. Mitochondrial oxidative stress as a novel therapeutic target to overcome intrinsic drug resistance in melanoma cell subpopulations. Exp Dermatol. 2015; 24:155–7. [PubMed: 25453510]
13. Roesch A, Vultur A, Bogeski I, Wang H, Zimmermann KM, Speicher D, et al. Overcoming intrinsic multidrug resistance in melanoma by blocking the mitochondrial respiratory chain of slow-cycling JARID1B(high) cells. Cancer Cell. 2013; 23:811–25. [PubMed: 23764003]
14. Zhang R, Zheng F. PPAR-gamma and aging: one link through klotho? Kidney Int. 2008; 74:702–4. [PubMed: 18756295]
15. Zhang H, Li Y, Fan Y, Wu J, Zhao B, Guan Y, et al. Klotho is a target gene of PPAR-gamma. Kidney Int. 2008; 74:732–9. [PubMed: 18547997]
16. Takada I, Kouzmenko AP, Kato S. PPAR-gamma Signaling Crosstalk in Mesenchymal Stem Cells. PPAR Res. 2010
17. Webster MR, Xu M, Kinzler KA, Kaur A, Appleton J, O'Connell MP, et al. Wnt5A promotes an adaptive, senescent-like stress response, while continuing to drive invasion in melanoma cells. Pigment Cell Melanoma Res. 2015; 28:184–95. [PubMed: 25407936]
18. Kaur AWM, Marchbank K, Behera R, Ndoye A, Kugel CH III, Dang VM, Appleton J, O'Connell MP, Cheng P, Valiga AA, Morissette R, McDonnell NB, Ferrucci L, Kossenkov AV, Meeth K, Tang H-Y, Yin X, Wood WH III, Lehrmann E, Becker KG, Flaherty KT, Frederick DT, Wargo JA, Cooper ZA, Tetzlaff MT, Hudgens C, Aird KM, Zhang R, Xu X, Liu Q, Bartlett E, Karakousis G, Eroglu Z, Lo RS, Chan M, Menzies AM, Long GV, Johnson DB, Sosman J, Schilling B, Schadendorf D, Speicher DW, Bosenberg M, Ribas A, Weeraratna AT. sFRP2 in the aged microenvironment drives melanoma metastasis and therapy resistance. Nature. 2016
19. The cancer genome atlas network: Genomic classification of cutaneous melanoma. Cell. 2015; 161:1681–1696. [PubMed: 26091043]
20. Usuda J, Ichinose S, Ishizumi T, Ohtani K, Inoue T, Saji H, et al. Klotho predicts good clinical outcome in patients with limited-disease small cell lung cancer who received surgery. Lung Cancer. 2011; 74:332–7. [PubMed: 21529984]
21. Lee J, Jeong DJ, Kim J, Lee S, Park JH, Chang B, et al. The anti-aging gene KLOTHO is a novel target for epigenetic silencing in human cervical carcinoma. Mol Cancer. 2010; 9:109. [PubMed: 20482749]
22. Wang L, Wang X, Jie P, Lu H, Zhang S, Lin X, et al. Klotho is silenced through promoter hypermethylation in gastric cancer. Am J Cancer Res. 2011; 1:111–9. [PubMed: 21969138]
23. Martin M, Marais R. Metformin: a diabetes drug for cancer, or a cancer drug for diabetics? J Clin Oncol. 2012; 30:2698–700. [PubMed: 22565000]

24. Aires V, Brassart B, Carlier A, Scagliarini A, Mandard S, Limagne E, et al. A role for peroxisome proliferator-activated receptor gamma in resveratrol-induced colon cancer cell apoptosis. Mol Nutr Food Res. 2014; 58:1785–94. [PubMed: 24975132]

25. Cerbone A, Toaldo C, Minelli R, Ciamporcero E, Pizzimenti S, Pettazzoni P, et al. Rosiglitazone and AS601245 decrease cell adhesion and migration through modulation of specific gene expression in human colon cancer cells. PLoS One. 2012; 7:e40149. [PubMed: 22761953]

26. Frohlich E, Wahl R. Chemotherapy and chemoprevention by thiazolidinediones. BioMed research international. 2015; 2015:845340. [PubMed: 25866814]

27. Kulke MH, Demetri GD, Sharpless NE, Ryan DP, Shivdasani R, Clark JS, et al. A phase II study of troglitazone, an activator of the PPARgamma receptor, in patients with chemotherapy-resistant metastatic colorectal cancer. Cancer journal. 2002; 8:395–9.

28. Botton T, Puissant A, Cheli Y, Tomic T, Giuliano S, Fajas L, et al. Ciglitazone negatively regulates CXCL1 signaling through MITF to suppress melanoma growth. Cell Death Differ. 2011; 18:109–21. [PubMed: 20596077]

29. Medici D, Razzaque MS, Deluca S, Rector TL, Hou B, Kang K, et al. FGF-23-Klotho signaling stimulates proliferation and prevents vitamin D-induced apoptosis. J Cell Biol. 2008; 182:459–65. [PubMed: 18678710]

Translational Relevance

Increasing klotho via PPARγ activation using rosiglitazone may provide new and effective strategies for the treatment of therapy-resistant melanoma in older patients. Our data indicate that, contrary to the majority of conventional therapies, alternate approaches that target age-associated molecules may be selectively effective in aged patients.

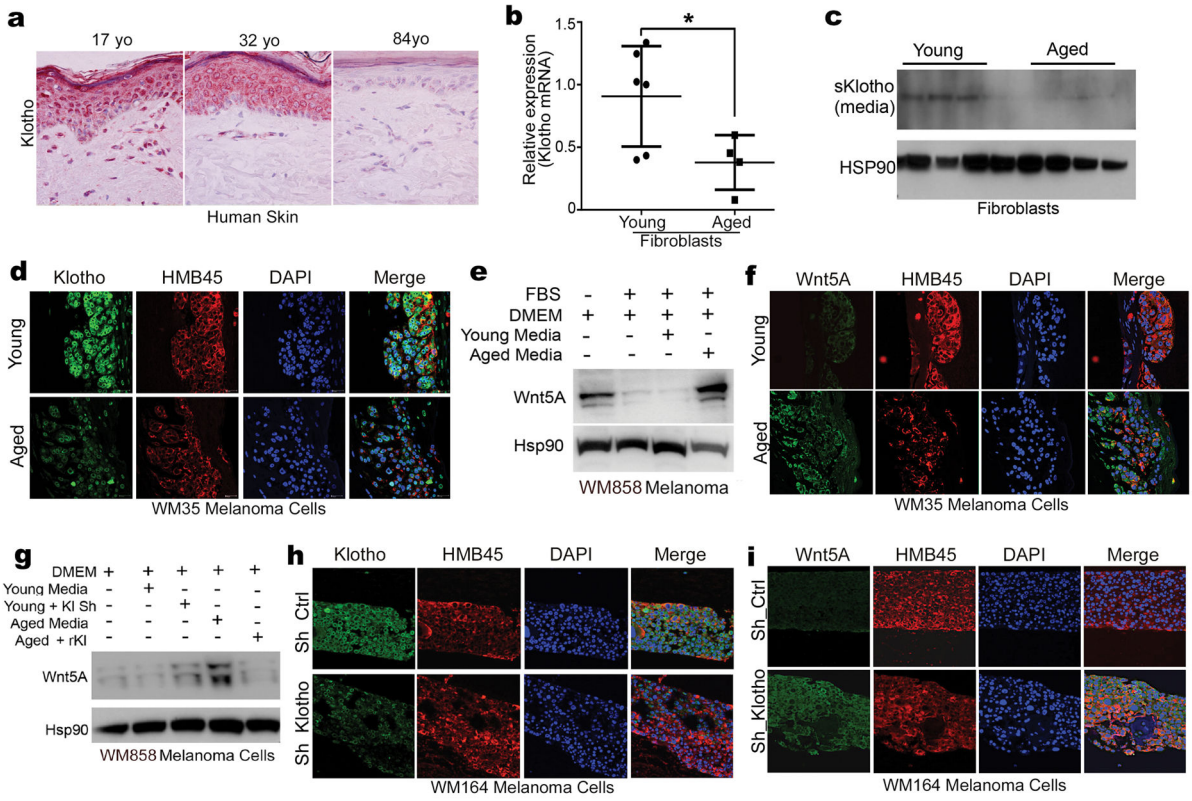

Figure 1. Loss of klotho in the aged microenvironment affects klotho and Wnt5A expression in melanoma cells

A, Immunohistochemical analysis of klotho in young and aged human skin (60X objective, 1X digital zoom). **B,** qRT-PCR of klotho mRNA in young (N=6) and aged (N=4) human fibroblasts (two-tailed unpaired t-test, p=0.04). **C,** Western analysis of klotho in the media of young and aged human fibroblasts. **D,** Immunofluorescent analysis of klotho (green), HMB45 (red) and Dapi (blue) expression in 3D organotypic skin reconstructs built with young or aged fibroblasts (63X objective)**. E,** Western analysis of Wnt5A in melanoma cells exposed to DMEM +/− serum, media from young fibroblasts or from aged fibroblasts. HSP90 was used as loading control**. F,** Immunofluorescent analysis of Wnt5A (green), HMB45 (red) and Dapi (blue) expression in 3D organotypic skin reconstructs built with young or aged fibroblasts (63X objective)**. G,** Western analysis of Wnt5A in melanoma cells exposed to media from young fibroblasts or young fibroblasts after klotho knock-down or aged fibroblasts +/− recombinant klotho. HSP90 was used as loading control**. H,** Immunofluorescent analysis of klotho (green) expression in 3D organotypic skin reconstructs built with young fibroblasts infected with either a control shRNA lentivirus or a sh_klotho lentivirus (63X objective). HMB45 (red) was used as melanoma cell marker and Dapi (blue) was used to stain nuclei**. I,** Immunofluorescent analysis of Wnt5A (green) expression in 3D organotypic skin reconstructs built with young fibroblasts infected with either a control shRNA lentivirus or a sh_klotho lentivirus (63X objective).

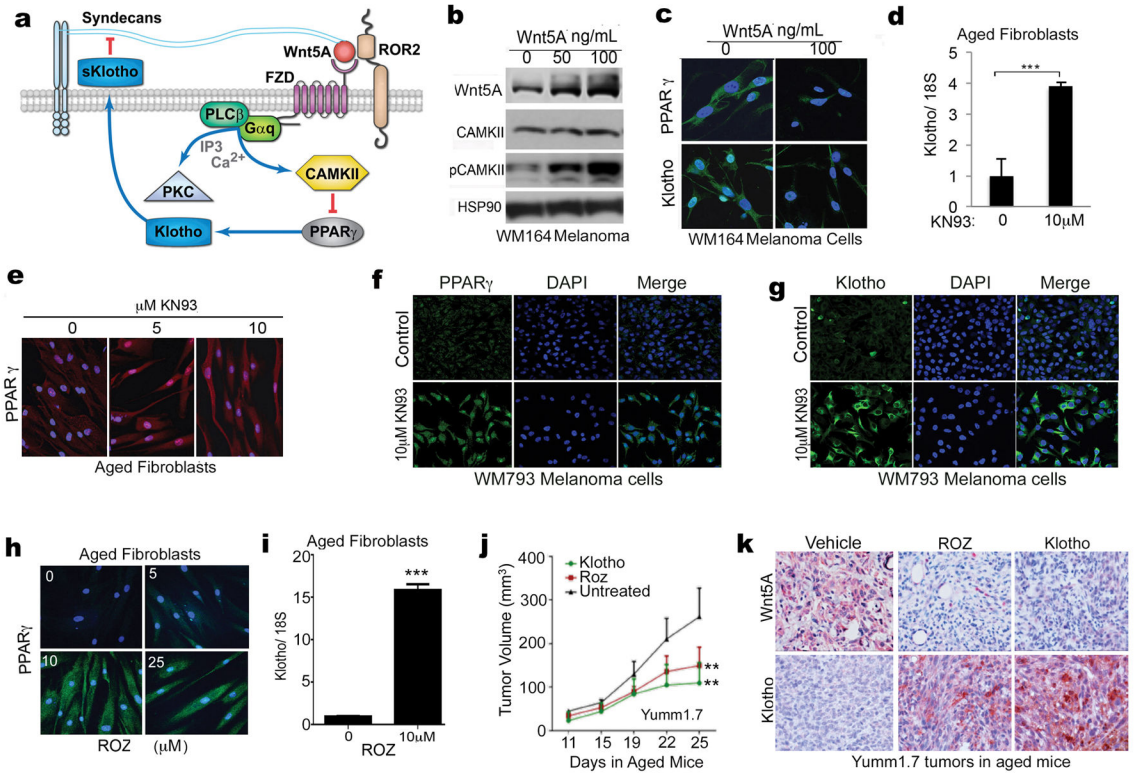

Figure 2. Wnt5A affects klotho expression via CAMKII mediated inhibition of PPARγ

A, Schematic of Wnt5A signaling showing activation of CAMKII, inhibition of PPARγ, and decrease of klotho transcription. Klotho is a sialidase and cleaves Wnt5A from syndecans at the cell surface, as we have previously published**. B,** Western analysis of active (phospho) and total CAMKII in melanoma cells treated with indicated dose of recombinant Wnt5A for 16h. **C,** Immunofluorescent analysis of PPARγ and klotho in melanoma cells treated with rWnt5A (63X objective). **D,**qRT-PCR analysis of klotho expression in aged fibroblasts treated with the CAMKII inhibitor KN93 (10μM, 48h) (two-tailed unpaired t-test, ***=p<0.001). **E,** Immunofluorescent analysis of PPARγ in KN93-treated aged fibroblasts (63X objective). **F,** Immunofluorescent analysis of PPARγ expression in melanoma cells after KN93 treatment (10μM, 48h) (63X objective). **G,** Immunofluorescent analysis of Klotho expression in melanoma cells after KN93 treatment (10μM, 48h) (63X objective). **H,** Immunofluorescent analysis of PPARγ expression in aged fibroblasts after treatment with PPARγ agonist Rosiglitazone (Roz) (63X objective). **I,** qRT-PCR analysis of klotho expression in aged fibroblasts treated with rosiglitazone (10μM, 48h) (two-tailed unpaired t-test, ***=p<0.001). **J,** Tumor growth curves of Yumm1.7 murine melanoma cells in aged C57/BL6 mice, in the presence of recombinant klotho (n=3), rosiglitazone (n=5), or vehicle control (n=4). Tumor burden was significantly less in mice treated with recombinant mouse klotho or rosiglitazone. Repeated measures analysis of variance (Anova) was calculated between samples. Holm Sidak correction was done, ***=p=0.0002 (Day-20). **K,** Analysis of Klotho and Wnt5A levels in mouse tumors by immunohistochemistry analysis after treatment with rosiglitazone or vehicle control (40X objective). Data represented as +/− SEM.

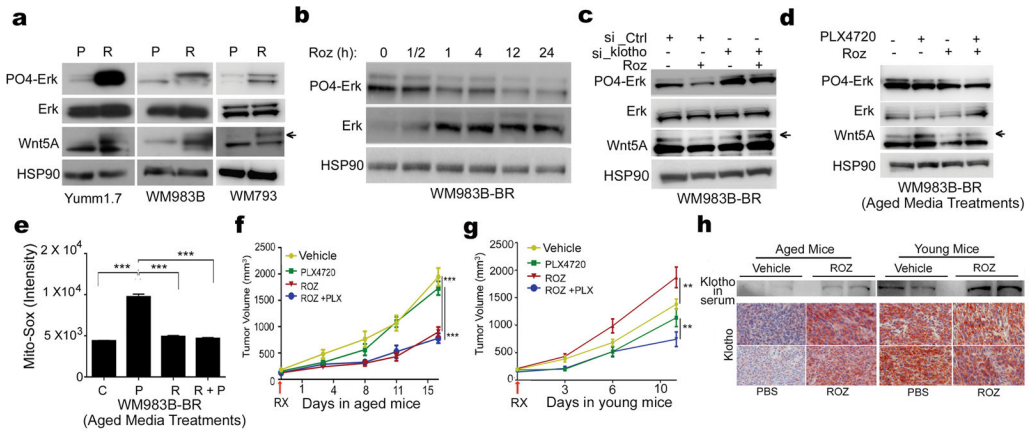

Figure 3. Rosiglitazone-mediated inhibition of phospho-Erk can inhibit growth of BRAF inhibitor resistant tumors

A, PO_4-Erk, Erk, and Wnt5A protein expression examined by western blot analysis in BRAF sensitive (Yumm1.7, WM983B, WM793) and resistant subclones (Yumm1.7_BR, WM983B_BR, WM793_BR). **B,** Western blot analysis for PO_4-Erk and Erk protein expression in WM983b_BR cells after treatment with rosiglitazone (10μM) for the indicated time period. **C,** Expression of PO_4-Erk, Erk and Wnt5A following treatment with rosiglitazone in WM983b_BR cells transfected with Ctrl or Klotho siRNA. **D,** PO_4-Erk, Erk, and Wnt5A protein expression examined by western blot analysis in WM983B-BR cells in the presence or absence of PLX4720 in conditioned media of aged fibroblasts treated with +/− rosiglitazone. **E,** Operetta® analysis of mito-SOX intensity (measurement of mitochondrial ROS) in WM983B_BR cells in the presence or absence of PLX4720 in conditioned media of aged fibroblasts treated with vehicle i.e. DMSO:PBS (1:10) or rosiglitazone (Anova $p<0.0001$; two tailed unpaired t-test, ***=$p<0.001$). C=control; P=plx4720; R= rosiglitazone; R+P= Rosiglitazone + plx4720. **F,** Tumor growth of BRAFi resistant Yumm1.7BR cells in aged (52 weeks) C57/BL6mice, +/− PLX4720 and +/− rosiglitazone. N=5 mice/group. Repeated measures analysis of variance (Anova) was calculated between samples, $p<0.0001$. Holm Sidak correction was performed, ***=$p<0.005$ (Day-18). **G,** Tumor growth of BRAFi resistant Yumm1.7BR cells in young (8 weeks) C57/BL6mice, +/− PLX4720 and +/− rosiglitazone (N=7 mice/group. Repeated measures analysis of variance (Anova) was calculated between samples, $p<0.0001$. Multiple comparision with Holm Sidak correction was done. **H,** Klotho levels in aged (left two panels) or young (right two panels) mouse serum (western blot) or tumors (immunohistochemistry) after treatment with rosiglitazone or vehicle control (40X objective).